# Implementing Conditional Re-illumination for Low-Damage Electron Microscopy

A. Agarwal<sup>1</sup>, J. Simonaitis<sup>1</sup>, N. Abedzadeh<sup>1</sup>, V. Goyal<sup>2</sup> and K. K. Berggren<sup>1</sup>

<sup>1</sup>Massachusetts Institute of Technology, Cambridge, USA <sup>2</sup> Boston University, Boston, USA E-mail: akshayag@mit.edu

## Introduction

Adaptive imaging techniques have been increasingly used in transmission and scanning electron microscopy, particularly in applications where low electron dose is necessary [1-3]. Recently, we introduced an adaptive imaging scheme that conditionally re-illuminates sample pixels based on the electron counts already collected at the electron imaging detectors [4]. Combined with interaction-free imaging [5], this scheme could potentially reduce the required imaging dose by an order of magnitude. However, our analysis was limited to opaque-and-transparent samples, and did not account for semi-transparency of the sample. In this work, we will develop the formalism for applying conditional re-illumination to semi-transparent samples. We will also discuss progress in experimental implementation of conditional re-illumination in an SEM.

#### **Methods**

We can treat the transparency  $\alpha \in [0,1]$  of a sample as a continuous random variable. We used the counts at the imaging detectors to form an estimate of  $\alpha$ , and analyzed the performance of the estimator by looking at its mean squared error (MSE). For unbiased estimators, the inverse of the classical Fisher Information (FI) forms a lower bound for this MSE (Cramér-Rao (CR) bound). We compared the performance of IFM and STEM by calculating the MSE for different estimators of  $\alpha$ , and comparing it to the CR bound.

A major requirement in implementing conditional re-illumination is the ability to count detected electrons. We outcoupled the signal from the Everhart-Thornley (ET) secondary electron detector of a Zeiss LEO SEM, using a 50  $\Omega$  impedance line onto a 2 GHz oscilloscope, and recorded the signal pulses. To obtain these pulses, the electron beam was held stationary and the ET signal recorded. Then, we created a histogram of the pulse heights, from which we hope to determine the signal level corresponding to single secondary electrons. Similar techniques have been previously used to count secondary electrons in SEM [6] and scattered electrons in STEM [7-9].

### Results

We found that the FI per incident electron on the sample was identical for STEM and IFM, shown by the solid blue curve in figure 1(a), (STEM imaging) and figure 1(b) (IFM imaging). Figure 1(a) shows the MSE of two STEM estimators for  $\alpha$ :  $\widehat{\alpha_1}$  and  $\widehat{\alpha_2}$ , calculated using Monte-

Carlo simulations. These estimators use the counts from the STEM imaging detectors (dark-and bright- field) in different ways -  $\widehat{\alpha_1}$  (purple dashed curve) averages over these counts to estimate  $\alpha$ , while  $\widehat{\alpha_2}$  (orange dashed-dotted curve) uses the ratio between the counts at the bright-field detector and the total counts at both detectors. Compared to  $\widehat{\alpha_1}$ ,  $\widehat{\alpha_2}$  has a lower MSE, and it meets the CR bound (solid blue curve). Figure 1(b) shows the MSE for two IFM estimators for  $\alpha$ :  $\widehat{\alpha_3}$  and  $\widehat{\alpha_4}$ .  $\widehat{\alpha_3}$  (purple dashed curve) averages over the counts at different IFM imaging detectors to estimate  $\alpha$ , while  $\widehat{\alpha_4}$  (orange dashed-dotted curve) uses the square of the difference between the counts. Again,  $\widehat{\alpha_4}$  is a better estimator for  $\alpha$  and is close to the CR bound.

Figure 2(a) shows the histogram of secondary electron pulse heights from the ET detector of a Zeiss LEO SEM. Since we held the beam stationary over a hole in the sample, the detector should nominally have no signal. The signal recorded on the detector can have two sources detector amplifier noise, and secondaries generated by the beam striking the walls of the microscope chamber. The histogram shows two peaks – a narrow peak at 0.4 V, which is also present when the gun is turned off, indicating that it is due to amplifier noise. A second, broad peak is present around 1.5 V. This peak is also present when the beam is held stationary over a thin carbon membrane, indicating that it arises due to secondaries. Such peaks have been previously attributed to the signal from single secondary electrons [5]. We are currently working on verifying the origin of this peak, and trying to obtain two- and three- electron peaks.

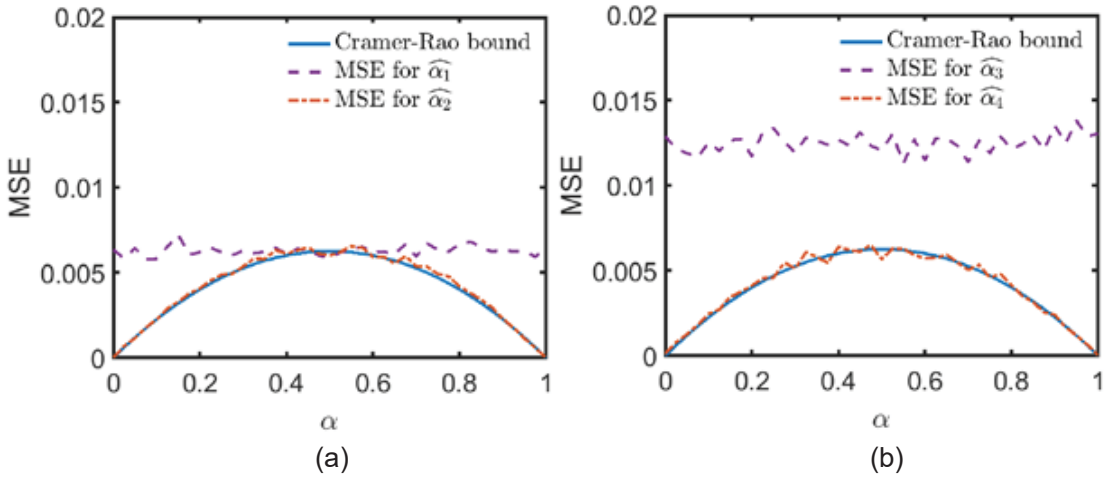


**Figure 1**: Mean square error (MSE) vs transparency  $\alpha$ , for (a) conventional STEM imaging, and (b) IFM imaging. MSE depends on how the estimators use the counts at various imaging detectors. This analysis is important for establishing the best estimator for the pixel transparency.

#### Conclusions

We are developing theoretical tools to analyze the information and error probability in semi-transparency measurements using STEM and IFM. We have also outcoupled the secondary electron signal from the ET detector on an SEM. If the histogram peak we have observed can be attributed to single secondaries, we can use its voltage level to count the number of secondaries produced on every sample pixel as the beam scans over it. This count would then

be used to infer the pixel's brightness (or transparency) using the estimators developed here, and a decision on re-illumination made using the expected MSE for the estimators developed in this work. Future work towards the implementation of conditional re-illumination for semi-transparent samples will entail refining these tools to account for loss of signal due to imperfect detection, and implementing customized scanning protocols to control the position of the beam (similar to vector scanning in electron beam lithography) and the pixel dwell time.

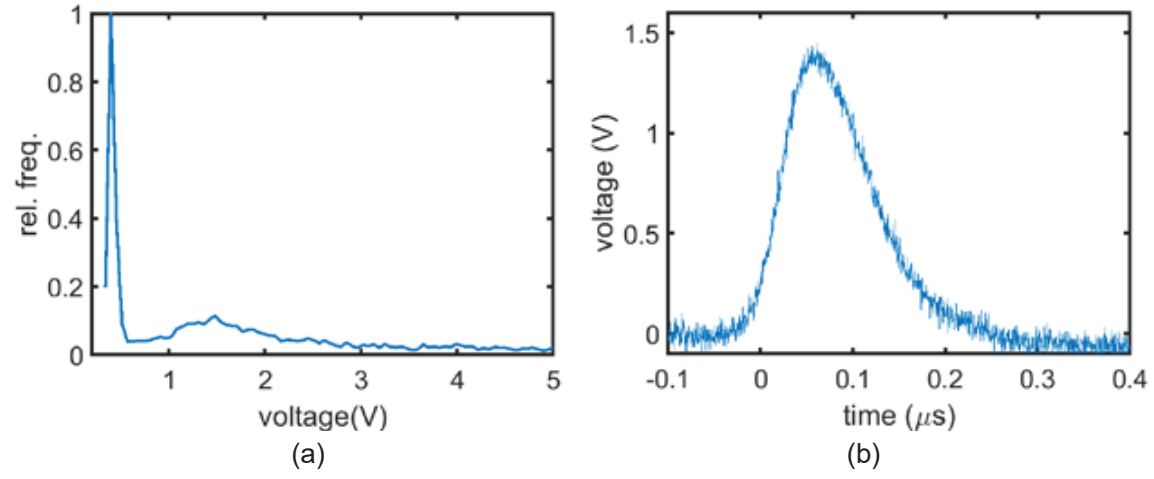


**Figure 2**: Outcoupling signal from ET detector on SEM. (a) Histogram of secondary electron pulse heights, showing a sharp peak near 0.4V due to amplifier noise, and a broad peak at 1.5V, possibly due to single electron pulses. (b) Example of a signal pulse that contributes to the broad peak.

### References

- [1] Stevens et al. (2018), Applied Physics Letters, **112**, 043104
- [2] Trampert et al. (2018), Ultramicroscopy, **191**, 11–17
- [3] Dahmen et al. (2016), Scientific Reports, **6**, 25350
- [4] Agarwal et al. (2019), arXiv:1901.09702 [physics.ins-det]
- [5] Elitzur and Vaidman (1993), Foundations of Physics, 23(7), 987–997
- [6] Uchikawa et al. (1992), Journal of Electron Microscopy, 41(4), 253–260
- [7] Ishikawa et al. (2014), Microscopy and Microanalysis, 20, 99–110
- [8] Mittelberger et al. (2018), Ultramicroscopy, **188**, 1–7
- [9] Sang at al. (2016), Ultramicroscopy, **161**, 3–9